Molecular Crystals and Liquid Crystals Science and Technology. Section A. Molecular Crystals and Liquid Crystals
Publication details, including instructions for authors and subscription information:
http://www.tandfonline.com/loi/gmcl19

Optical-DC-Field Induced Space Charge Fields and Photorefractive-Like Holographic Grating Formation in Nematic Liquid Crystals

I. C. Khoo [a]

[a] Electrical Engineering Department, The Pennsylvania State University University Park, PA, 16802

Version of record first published: 24 Sep 2006.

To cite this article: I. C. Khoo (1996): Optical-DC-Field Induced Space Charge Fields and Photorefractive-Like Holographic Grating Formation in Nematic Liquid Crystals, Molecular Crystals and Liquid Crystals Science and Technology. Section A. Molecular Crystals and Liquid Crystals, 282:1, 53-66

To link to this article: http://dx.doi.org/10.1080/10587259608037568

Mol. Cryst. Liq. Cryst., 1996, Vol. 282, pp. 53–66
Reprints available directly from the publisher
Photocopying permitted by license only

OPTICAL-DC-FIELD INDUCED SPACE CHARGE FIELDS AND PHOTOREFRACTIVE-LIKE HOLOGRAPHIC GRATING FORMATION IN NEMATIC LIQUID CRYSTALS

I. C. KHOO
Electrical Engineering Department
The Pennsylvania State University
University Park, PA 16802

Abstract We present a detailed theoretical discussion of the fundamental mechanisms for dc field assisted optically induced space charge fields and molecular reorientation effects in nematic liquid crystal films. In fullerene C_{60}-doped film, persistent director axis reorientation is observed, allowing the recording of holographic and other optical phase gratings.

INTRODUCTION

Nematic liquid crystal director axis reorientation by an optical field with or without the aid of low frequency or dc electric/magnetic field has been investigated by many workers for almost two decades [1-4]. It is well known by now that these processes result in large refractive index changes with the use of low power lasers. In some dye-doped nematic films almost two orders of magnitude improvement in the nonlinear response was achieved by Janossy et al. [5] and others [6]. The enhancement is attributed to molecular torque exerted by the photo-excited dye dopant molecules on the nematic liquid crystal molecules. The molecular torque, Γ_m arising from [dc] intermolecular fields is larger than those exerted by the optical field Γ_{op}, i.e., $\Gamma_m = \eta\Gamma_{op}$ (with $\eta >> 1$), because of several factors; one obvious factor is the largeness of the dc dielectric anisotropy $\Delta\epsilon = \epsilon_\parallel - \epsilon_\perp$ compared to the optical anisotropy $(\Delta\epsilon)_{op} = \epsilon_\parallel^{op} - \epsilon_\perp^{op}$. Typically, $\Delta\epsilon \sim 5$ whereas $\Delta\epsilon^{op} \approx 0.5$.

Recently, we have [7] revisited the process of dc field assisted optically induced molecular reorientation effects in nematic liquid crystal film, and observed a new class of electro-optical process that yields by far the largest known optical nonlinearity in nematic liquid crystal film. The effects were observed in undoped or lightly doped film of high transparency, in contrast with the heavily absorbing dye-doped systems [5, 6]. Similar results have also been obtained by Rudenko and Sukhov [8], who attributed the effect to a photorefractive-like space charge field [9] arising from the photoinduced conductivity anisotropy. On the other hand, our experiments and theoretical analysis show that space charge field arising from conductivity and dielectric anisotropies as well, the well-known Carr-Helfrich effect [10].

DC SPACE CHARGE FIELDS, TORQUES AND DIRECTOR AXIS REORIENTATIONS

The field-nematic liquid crystal interaction configuration is depicted in figure 1. Experimental evidence and our recent theoretical analyses [11] have shown that these observed effects involve the following processes and scenario as schematically depicted in figure 2.

(i) Charge generation → ions drift/diffusion → charge separation and space charge field formation → director axis reorientation → refractive index change.

(ii) Charge generation → ionic conduction plus director axis reorientation → space charge field formation through dielectric and conductivity anisotropies → further director axis reorientation → refractive index change.

(iii) Charge generation → material flows → velocity gradient and shear stresses → director axis reorientation → refractive index change.

Process (i) is analogous to those occurring in photorefractive crystals [9]. Following photo-charge production, space charges and dc fields are set up through diffusion, ion drifts and recombination processes.

The photorefractive-like space charge field $\vec{E}_{ph}$ due to photo-induced conductivity (ionic) inhomogeneity is given by [8]:

$$E_{ph} = \frac{mk_BT}{2e} q v \frac{\sigma - \sigma_d}{\sigma} \sin(\vec{q} \cdot \vec{r}) \tag{1}$$

$$= E_{ph}^{(0)} \sin q\xi$$

where k_B = Boltzman constant, σ = illuminated state conductivity, σ_d = dark state conductivity, $v = \frac{D^+ - D^-}{D^+ + D^-}$ where D^+ and D^- are the diffusion constants for the positively and negatively charged ions, respectively. Notice that E_{ph} is $\pi/2$ phase shifted from the optical grating function (and m is the modulation ratio in the input optical intensity $I_{op} = I_0(1 + m\cos(\vec{q} \cdot \vec{r}))$. This $\pi/2$ phase shift is responsible for the two-beam coupling effect reported in reference [7].

Processes (ii) and (iii) are unique to nematic liquid crystals (NLC), and are simply due to the fact that the director axis of the uniaxial birefringence NLC could be reoriented by the fields present. In combination with the anisotropies in

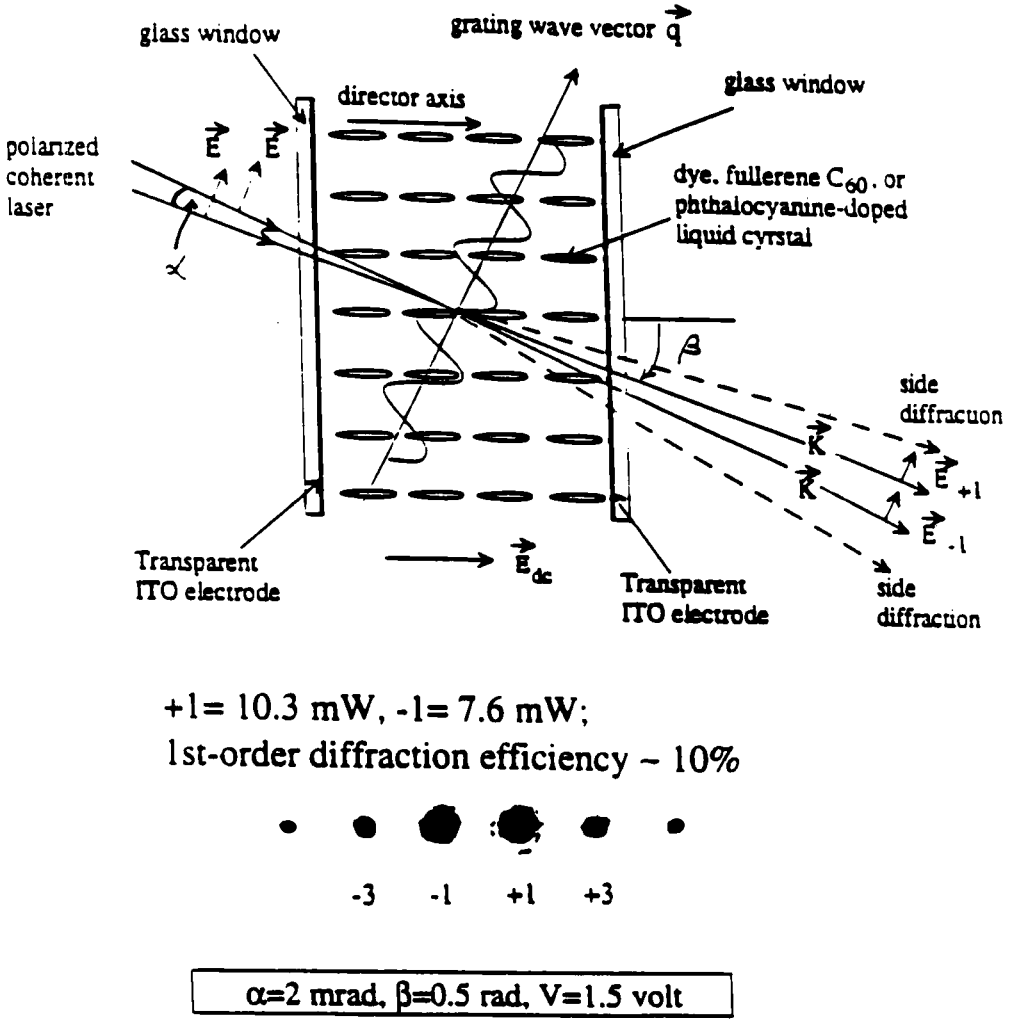

Figure 1 Schematic depiction of the interacting fields in a nematic liquid crystal film. +3 and -3 are first order self-diffractions from the grating generated by the incident +1 and -1 beam.

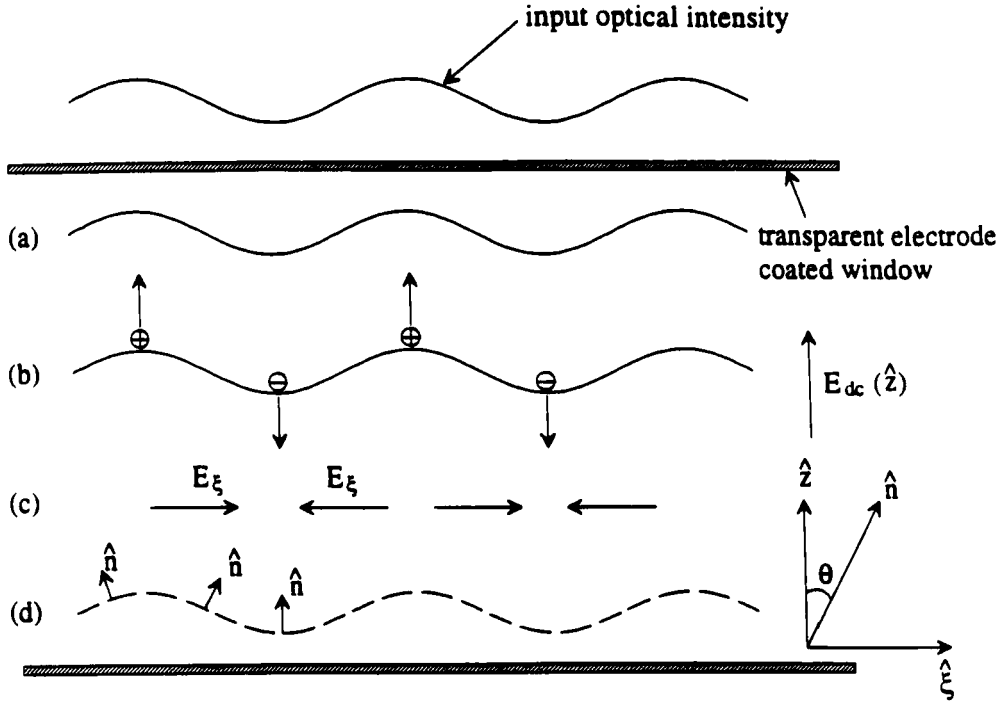

Figure 2 Spatial distribution of various parameters involved in the nonlinear photorefractive effects. (a) photoinduced conductivity modulation (b) flow velocity and space charges, (c) dc space charge fields, (d) director axis reorientation profile ($\hat{n}$ is normal to the dotted line; θ is the reorientation angle).

conductivity and dielectric constants, space charges and dc fields are formed [10, 11]. For the geometry depicted in figure 2, these space charge fields can be shown to be:

$$E_{\xi,\sigma} = \frac{-(\sigma_{\parallel} - \sigma_{\perp})\cos\theta\sin\theta}{\sigma_{\parallel}\sin^2\theta + \sigma_{\perp}\cos^2\theta}E_z \sim \frac{\Delta\sigma}{\sigma_{\perp}}\theta E_z \text{ (for small } \theta) \tag{2a}$$

and

$$E_{\xi,\epsilon} = \frac{-(\epsilon_{\parallel} - \epsilon_{\perp})\cos\theta\sin\theta}{\epsilon_{\parallel}\sin^2\theta + \epsilon_{\perp}\cos^2\theta}E_z \sim \frac{-\Delta\varepsilon}{\varepsilon_{\perp}}\theta E_z \text{ (for small } \theta) \tag{2b}$$

where $\Delta\sigma = \sigma_{\parallel} - \sigma_{\perp}$ is the conductivity anisotropy and $\Delta\epsilon = \epsilon_{\parallel} - \epsilon_{\perp}$ the dc dielectric anisotropy.

Notice that these space charge fields are proportional to the applied dc field E_z, i.e., larger applied dc field will create larger space charge field. Secondly, the magnitude of these space charge fields are an increasing function of the induced reorientation angle θ, for small ϑ. A small initial reorientation angle and space charge field will thus reinforce each other; once the reorientation is established, we can see from equations (2a) and (2b) that the space charge fields can be maintained by simply applying the dc field, without participation from the incident optical field at all. Such effect was observed in our reported study [11] of the holographic grating formation dynamics.

All three processes outlined above involve the basic mechanism of photo-charge production. Since the incident photonic energy $h\nu$ is less than the ionization potentials of the dopant and the impurities molecules in the liquid crystals, the photo-charge productions are attributed to excited state photochemical processes. In the case of R6G dye or other laser dye molecules, studies [8] have shown that the ions are generated by dissociation, whereas in C_{60} molecules, the formation of charge transfer complexes [12] is the likely cause. Some hitherto undetermined electro-chemical processes may also play a role in the persistent holographic process, as evidenced by the observed difference in the grating storage time. In R6G dye doped sample, the written grating lasts for tens of minutes, whereas grating written in C_{60}-doped sample persists indefinitely. A series of preliminary investigations involving various laser dyes (R6G, methyl red, phthalocyanine-based laser dye, dichroic dyes D2, D16 [5, 6], and C_{60} have shown that indeed the photo-charge production yield is characteristic of the molecules excited structures, and is not correlated with the ground-state absorption rate. For example, the dichroic dye D2 and D16 doped NLC films is highly absorptive ($\alpha > 100$ cm^{-1}) but yields small photocurrent and vanishing electro-optical effect in contrast to the lightly absorbing C_{60} doped liquid crystals ($\alpha \lesssim 20$ cm^{-1}).

The dynamics of the director axis reorientation process, is governed by interplay among the various torques produced by the fields present and the elasticity of the liquid crystals. The principal torques involved are the dielectric torque $\tau_{\Delta\epsilon}$, the

flow-shear stress torque τ_{flow} and the elastic restoring torque τ_{el}. For the geometry depicted in figure 2, these torques are given respectively by:

$$\tau_{\Delta\varepsilon} = \frac{\Delta\varepsilon}{4\pi}\left[\sin\theta\cos\theta\ (E_\xi^2 - E_z^2) + \cos 2\theta\ E_\xi E_z\right], \tag{3a}$$

where E_ξ and E_z are the ξ- and z- component of the total dc electric field $\vec{E}_{dc}$:

$$\vec{E}_{dc} = E_z\hat{z} + \vec{E}_{\xi,\sigma} + \vec{E}_{\xi,\varepsilon} + \vec{E}_{ph}; \tag{3b}$$

$$\tau_{flow} = -\frac{dV(\xi)}{d\xi}[\alpha_3\cos^2\theta - \alpha_2\sin^2\theta] \tag{4}$$

where α_2 and α_3 are the Leslie coefficient;

$$\tau_{el} = [K_1\sin^2\theta + K_3\cos^2\theta]\frac{d^2\theta}{dz^2} + [(K_1 - K_3)\sin\theta\cos\theta]\left[\frac{d\theta}{dz}\right]^2 \tag{5}$$

$+$ ... similar terms in $\frac{d^2\theta}{d\xi^2}$ and $\frac{d\theta}{d\xi}$

The dynamics of the reorientation process is described by the equation

$$\tau_{\Delta\varepsilon} + \tau_{flow} + \tau_{el} + \tau_{op} + \gamma\frac{d\theta}{dt} = 0 \tag{6}$$

where γ is an appropriate interaction-geometry dependent viscosity coefficient.

In the steady state $[\dot{\theta} = 0]$, the torque balance equation, for small reorientation and assuming one elastic constant approximation for simplicity, becomes

$$K\left[\frac{\partial^2\theta}{\partial z^2} + \frac{\partial^2\theta}{\partial\xi^2}\right] + \frac{\Delta\varepsilon}{4\pi}E_a E_{ph}^{(0)}\cos\beta\ \sin q\xi$$

$$+ \frac{\Delta\varepsilon}{4\pi}E_z^2\left[1 + \frac{\alpha_3}{\eta_2}\frac{\Delta\sigma}{\sigma_\parallel}\frac{\varepsilon_\perp}{\Delta\varepsilon} + \left(\frac{\Delta\varepsilon}{\varepsilon_\perp} + \frac{\Delta\sigma}{\sigma_\perp}\right)\cos\beta\right]\theta = 0 \tag{7}$$

where we have retained the largest among all contributing terms to first order in θ. In deriving equation (7), we have rewritten the flow-orientation torque τ_{flow} as

$$\tau_{flow} = \frac{\alpha_3}{\eta_2}\left[\frac{\Delta\sigma}{\sigma_\parallel}\right]\frac{\varepsilon_\perp}{4\pi}E_z^2 \cdot \theta \tag{8}$$

by applying the Poisson's equation:

$$\frac{\partial E_\xi}{\partial \xi} = \frac{4\pi\rho_{sc}}{\varepsilon_\perp} \tag{9a}$$

the equation of continuity:

$$\text{div. } I_x = 0 \tag{9b}$$

where $I_x = \sigma_\parallel E_x + \Delta\sigma E_z\theta$.

and the viscous force equation:

$$\rho_{sc}E_z = \eta\frac{\partial}{\partial\xi}\left[\frac{\partial V(\xi)}{\partial\xi}\right] \tag{9c}$$

Writing θ as $\theta=\theta_0\sin(\frac{\pi z}{d})\sin q\xi,$, equation (7) can be solved to give

$$\theta_0 = \frac{\Delta\varepsilon E_z E_{ph}^{(0)}\cos\beta}{K[\frac{\pi^2}{d^2} + q^2] + \frac{\Delta\varepsilon E_z^2}{4\pi}[1 + (\frac{\Delta\varepsilon}{\varepsilon_\perp} + \frac{\Delta\sigma}{\sigma_\perp})\cos\beta + \frac{\alpha 3}{\eta_2}\frac{\Delta\sigma}{\sigma_\parallel}\frac{\varepsilon_\perp}{\Delta\varepsilon}]} \tag{10}$$

DYNAMICS

The nematic liquid crystal used in our wave mixing experiment is 5CB (Pentyl-Cyano-Biphenyl), doped with 0.2% or 0.05% by weight of R6G dye and Fullerene C_{60}, resulting in absorption constants (at λ = 5145Å Argon laser line) of 101 cm^{-1} and 30 cm^{-1} respectively. The film thickness is 25 μm. The input Ar^+-ion writing beams are electronically controlled to yield square pulses of variable duration to prove the dynamics and magnitude of the induced reorientation grating, a phase grating for the input extraordinary-polarized waves. The nature and time evolution of the grating, as monitored by the first order diffraction from an extraordinary-polarized probe laser is depicted in figure 3. If the illumination time is short ($\lesssim$ a few seconds), the induced grating is transient. The probe diffraction builds up to a quasi-steady-state value in

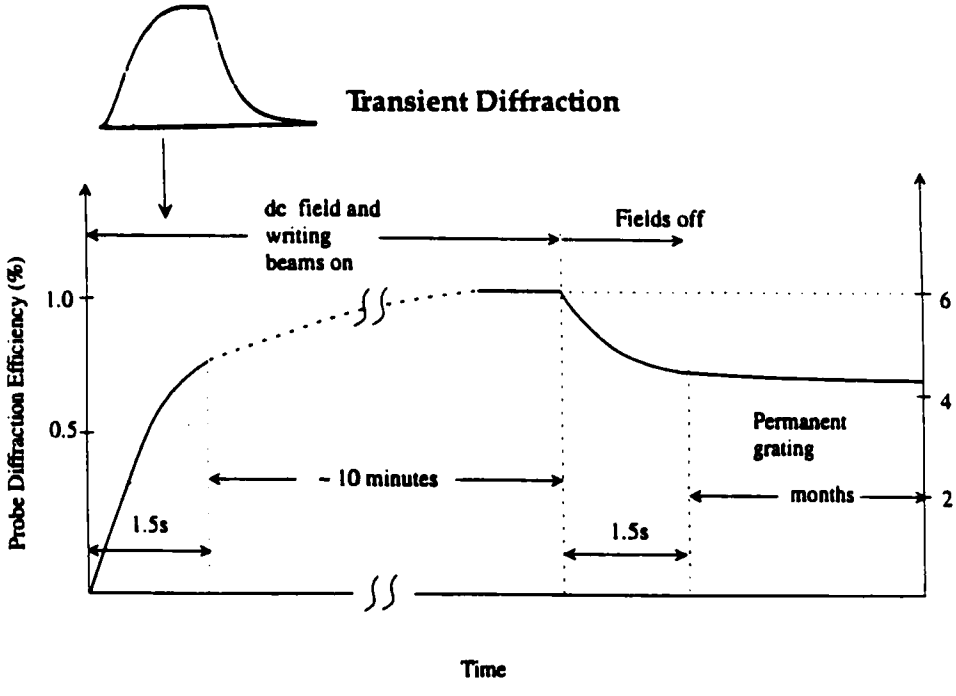

Figure 3 Schematic depiction of the dynamics of transient and permanent grating formation in a C_{60}-doped nematic liquid crystal film. Film thickness = 25 μm; α_{air} = 0.024 rad; β = 22.5°; +1 beam power = 32 mWatt; -1 beam power = 21 mWatt; V_{dc} = 1.5 Volt; C_{60} dopant concentration = 0.05% by weight. Insert shows an oscilloscope trace of transient grating diffraction from a 25 μm thick C_{60}-doped nematic film illuminated by 2-second long square pump laser pulses.

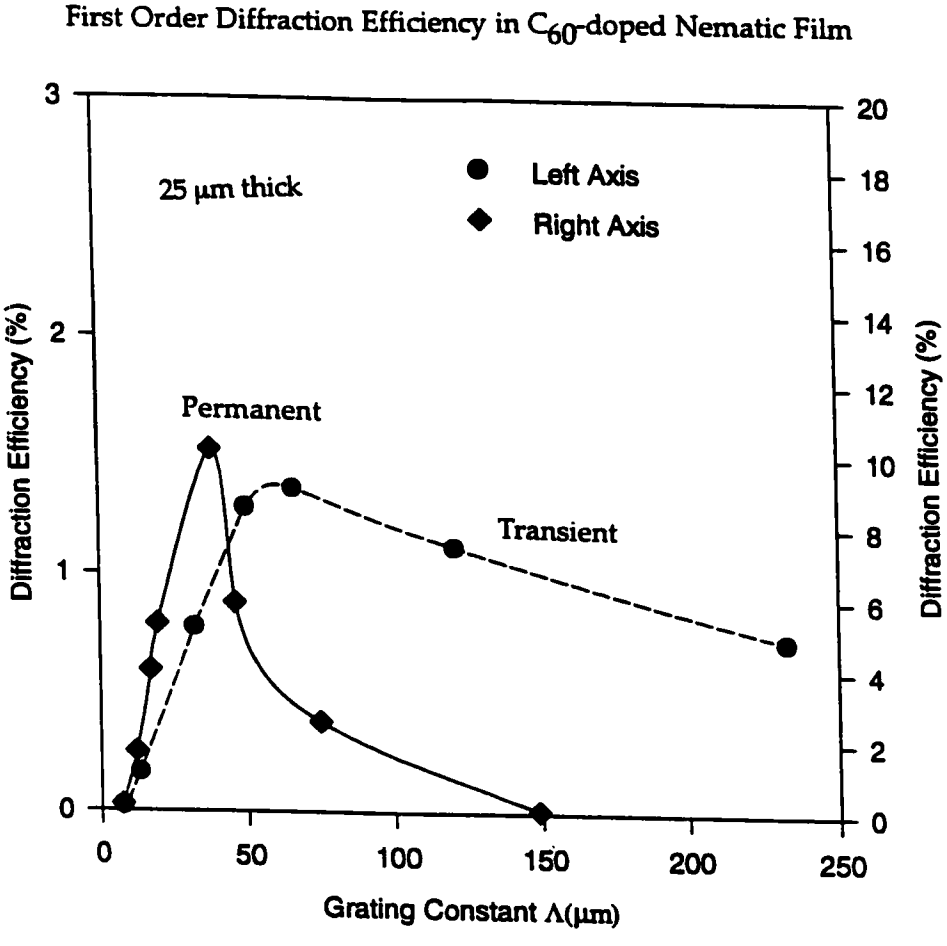

Figure 4 First order diffraction efficiency dependence on the grating constants for a 25 μm C_{60}-doped film. (a) Transient grating, (b) permanent grating. +1 beam power = 10 mWatt, -1 beam power = 7.6 mWatt.

$\lesssim$ 1 sec; when the input beams or fields are turned off, the grating decays to a vanishing value in $\lesssim$ 1 sec.

If the writing beams are kept on after the initial quasi-stationary value is reached, it is observed that the probe diffraction slowly but steadily increases in magnitude, before settling down to a final steady state value after 15-20 minutes. If the writing beams are turned off before the final steady state is reached, while the dc field is kept on, it is observed that the probe diffraction drops (in a second or so) to a lower but finite value.

This diffraction persists as long as the dc field is on, for tens of minutes. If the dc field is off, the diffraction decays to an even lower persistent value, depending on illumination time. We believe that at this stage, the reorientation angle θ has acquired a sufficiently large magnitude after prolonged optical illumination and applied field. The dc-applied field dependent space charge fields $E_{\xi,\sigma}$ (equation (2a)) and $E_{\xi,\epsilon}$ (equation (2b)) become explicitly substantial. Notice from equations (2a) and (2b) that these space charge fields depend explicitly on the reorientational angle and the dc-applied field, and not on the incident optical field, in contrast to the photorefractive space charge field E_{ph}. This explains why the reorientation can be sustained by the dc field with the writing beams turned off.

At the final stage of grating formation, strong diffuse scatterings and high order diffractions are observed; the diffraction efficiency is more than an order of magnitude larger than (in some cases, it can be 50 times larger) the initial "quasi-stationary" value observed in the transient stage. If all external applied (dc and optical) fields are turned off, a "persistent" grating remains. In R6G dye-doped film, the grating decays in a couple of hours. On the other hand, in Fullerene C_{60}-doped sample, the grating persists indefinitely. We believe that such persistent gratings are due to a irreversible perturbation of the surface director axis alignment by the current and nematic flows under prolonged application of the optical and dc fields.

Large and irreversible distortion of the director axis distortion can be induced in a shorter illumination time if higher-power writing beam and/or higher dc voltages are used. We have found that with a writing beam power on the order of 500 mWatt and a dc voltage of 10 V, permanent gratings of a few % in diffraction efficiency can be generated in a few seconds.

High optical power/dc applied voltage, however, usually results in grating with high degree of depolarization. This is due to the higher degree of turbulence and randomness in the director axis reorientation caused by the large current and nematic flows under high optical and dc fields. More quantitatively, consider the ratio of the first order diffraction efficiencies $R = \eta_{\parallel}/\eta_{\perp}$ ($\eta_{\parallel}$ and $\eta_{\perp}$; efficiencies for He-Ne polarization parallel and perpendicular to the Argon writing beams respectively). For low power (a few mWatts) writing beams and low dc voltage (1-2 volt) $R \approx 20$ whereas $R \approx 1$ (i.e., almost randomly polarized grating) for writing beams power around 10^2 mWatts and/or dc voltage of several volts.

An interesting and useful feature of these holographic gratings is that they can be electronically turned on and off, as the director axis of the liquid crystal responses to an applied ac field through the usual electro-optical effect [4]. We found that a

200 Hz, 94 Volt ac field will completely realign the whole sample, i.e., turn off the grating with a rather fast response time of 0.2 millisecond; when the ac field is removed, the grating will recover in a time of 20 milliseconds.

Through their different dependencies on θ and the applied dc and optical fields (c.f., equations 1-2), the space charge fields and the resulting reorientational torques come into play in a time dependent way. We note here one other interesting difference between the transient and the persistent grating, namely, their grating constant dependence as depicted in figure 4a-4b.

In the transient case, when θ is small, we expect that only the photorefractive-like space charge field will contribute, i.e., ignore the θ-dependent terms in equation 7. In that case, θ_0 is of the form

$$\theta_0 \sim q/K[\frac{\pi^2}{d^2} + q^2] \tag{11}$$

where the q dependence in the numerator comes from E_{ph}. This gives a maximum at $q \sim \frac{\pi}{d}$, i.e., at a grating constant $\Lambda_{max} = 2d$, in close agreement with $\Lambda_{max} \approx 55\ \mu m$ in figure 4a.

On the other hand, upon prolonged illumination by the writing beam, the reorientation angle θ dependent term in equation 7 will contribute significantly. In that case, θ_0 is of the form given in equation (10). Using the typical nematic 5CB parametric values: $\epsilon_\parallel = 15$, $\epsilon_\perp = 10$, $\sigma_\parallel = 6 \times 10^{-11}$ ohm^{-1} cm^{-1}, $\sigma_\perp = 4 \times 10^{-11}$ ohm^{-1} cm^{-1}, $K = 0.6 \times 10^{-6}$ dyne, $d = 25\ \mu m$, $V = 1.5$ Volt, the second square-bracketed term in the denominator is estimated to be of the same magnitude as $K\frac{\pi^2}{d^2}$. In other words, θ_0 is of the form $\theta_0 \sim \frac{q}{K(\frac{\pi^2}{d_*^2} + q^2)}$, where $2d_*^2 \approx d^2$. This gives a maximum at a grating constant $\Lambda_{max} \approx 1.414\ d \approx 35\ \mu m$. This is close to the experimental observed value, c.f., figure 4b.

In reference [11], we have also estimated the magnitudes of the three space charge fields. For the case of $\Lambda = 50\ \mu m$, $E_z = 600$ V/cm (1.5 volt in 25 μm), we get $E_{\xi,\sigma} \sim 2.4$ V/cm, $E_{\xi,\epsilon} \sim 9.6$ V/cm and $E_{ph} \sim 13$V/cm, for an input optical intensity on the order of 0.6W/cm^2. Notice that these fields, while small in magnitude, gives much large dielectric torques when combined with large dc anisotropy ($\Delta\epsilon \approx 5$) and the applied dc field E_z. For these three fields, the dielectric torques $\tau_{\Delta\epsilon} \sim \Delta\epsilon E_z E_{sc}$ (E_{sc} = space charge field) are on the order of 7.2×10^3 (V/cm^2), 2.88×10^4 (V/cm)^2, and 3.9×10^4 (V/cm)^2, respectively. On the other hand, an optical intensity of 0.6 W/cm^2 will give an optical torque $(\Delta\epsilon)_{op}E_{op}^2$ on the order of 3×10^2(V/cm)^2, which is 1 to 2 orders of magnitude smaller. In other words, the optical-dc-field induced reorientation torques giving rise to the effects

reported here for very lightly absorbing NLC film is comparable in magnitude to the molecular torque [5, 6] in heavily absorbing dyed doped system, c.f., the discussion in the introduction section.

As one may note from figure 4b, the first order diffraction efficiency $\eta \approx$ 10% at Λ_{max}. Since $\eta \sim (\Delta n \pi d/\lambda)^2$ for thin grating, this corresponds to $\Delta n \sim 2 \times 10^{-3}$. On the other hand, F ~ (0.01 Watt) x 600 sec/(0.3cm)^2 = 60J/cm^2). Therefore, the nonlinear sensitivity S/ as defined in [13], S = $\Delta n/F$ obtained in our preliminary study here is on the order of 3 x 10^{-5} cm^2/J. This value of S is already comparable to those obtainable from photorefractive material [9] and hydrogen treated germano-silicate glass [13]. Clearly, by using nematic liquid crystals in which higher concentration of C_{60} could be dissolved, and or different (shorter) writing beam wavelength (c.f., absorption curve of C_{60} dissolved in liquid crystal as shown in figure 5), the nonlinear sensitivity can be improved. Because of their broadband birefringence and transparency [from visible through the near-and mid-IR spectral regime, i.e., 0.4 μm - 5 μm], and extraordinary electro-optical response, liquid crystal films have been widely used in various image processing, storage and display devices and systems [4]. This study shows that they are promising candidates for electro-optical holographic storage applications as well. Studies along these lines are currently underway.

ACKNOWLEDGEMENT

This research is supported in part by the Air Force Phillips Laboratory and the Army Research Office. I am indebted to Bob D. Guenther for some helpful technical discussion and suggestions, and to Y. Liang, H. Li and K. Wang for some technical assistance in data collection.

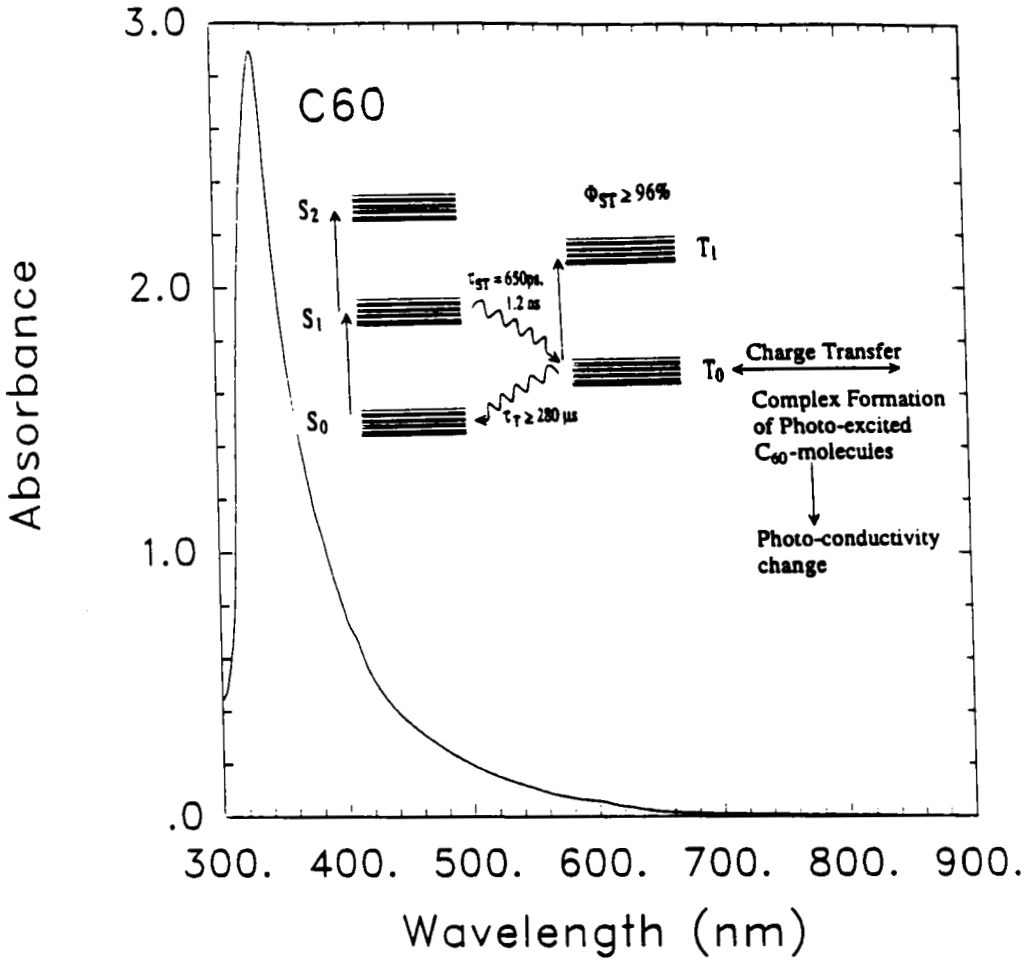

Figure 5 Measured absorbance of C_{60} dissolved in liquid crystal. Insert shows the energy levels and possible intra-molecular processes leading to charge transfer complex formation after photoexcitation from S_0 to S_1 state.

REFERENCES

1. R. M. Herman and R. J. Serinko, Phys. Rev. A19, 1757 (1979).
2. S.-H. Chen and J. J. Wu, Appl. Phys. Lett. 52, 1998 (1988) and references therein on earlier publications.
3. N. V. Tabiryan and B. Ya Zeldovich, Mol. Cryst. Liq. Cryst. 62, p. 637; 69, p. 19; 69, p. 31 (1981).
4. I. C. Khoo, "Liquid Crystals: Physical Properties and Nonlinear Optical Phenomena," Wiley Interscience, NY (1994). See also I. C. Khoo and S. T. Wu, "Optics and Nonlinear Optics of Liquid Crystals," World Scientific, Singapore (1993).
5. I. Janossy, L. Csillag and A. D. Lloyd, Phys. Rev., A44, p. 8410 (1991); I. Janossy and T. Kosa, Opt. Lett. 17, 1183 (1992).
6. I. C. Khoo, H. Li and Y. Liang, IEEE J. Quant. Electron. JQE29, 1444 (1993).
7. I. C. Khoo, H. Li and Y. Liang, Opt. Lett. 19, 1723 (1994).
8. E. V. Rudenko and A. V. Sukhov, JETP Letts. 59, p. 142 (1994); JETP 78, p. 875 (1994).
9. See, for example, P. Yeh, "Introduction to Photorefractive Nonlinear Optics," Wiley Interscience, NY (1993).
10. W. Helfrich, J. Chem. Phys. 51, p. 4092 (1969); see also P. G. deGennes and J. Prost, "The Physics of Liquid Crystals," Oxford University Press, NY (1993).
11. I. C. Khoo, Opt. Lett (Oct. issue, 1995).
12. Y. Wang and L. T. Cheng, J. Phys. Chem. 96, 1530 (1992); Y. Wang, J. Phys. Chem. 96, 764 (1992).
13. See, for example, A. Partovi, T. Erdogan, V. Mizrahi, P. J. Lemaire, A. M. Glass and J. W. Heming, Appl. Phys. Lett. 64, 821 (1994).